DOI: http://doi.org/10.5281/zenodo.15744674

A Comparative Study on the Wear Behaviour of TiN, TiAlN, and TiAlSiN Coatings on X100CrMoV5 Steel

Elif BAŞER
Graduate School of Natural and Applied Sciences, Ege University
baserelif4@gmail.com, ORCID: https://orcid.org/ 0009-0002-7125-9901

Ege Anıl DİLER
Department of Mechanical Engineering, Ege University
ege.anil.diler@ege.edu.tr, ORCID: https://orcid.org/0000-0002-1667-5737

Abstract

This study investigated the wear behaviour of TiN, TiAlN, and TiAlSiN-coated X100CrMoV5 steels, using physical vapour deposition, under a range of applied loads (2 N, 6 N, and 10 N) and sliding speeds (0.1 m/s, 0.2 m/s, and 0.3 m/s). Hardness measurements revealed a progressive increase in hardness from TiN to TiAlN, with TiAlSiN exhibiting the highest value, directly correlating with the wear performance. The TiAlN and TiAlSiN coatings achieved hardness values that were approximately 1.36 and 1.6 times greater than that of the TiN coating, respectively. Statistical analysis utilizing regression modelling and ANOVA demonstrated a strong and significant influence of both load and sliding speed, as well as their interaction effect, on the wear rate for all coatings. Notably, the applied load exerted a more substantial impact on the wear rate compared to the sliding speed. The results of wear tests indicated that the TiAlSiN coating consistently yielded the lowest wear rate, signifying a significant enhancement in the wear resistance of the X100CrMoV5 steel. The findings underscore the potential of TiAlSiN coatings as a highly effective surface modification strategy for improving the durability and extending the lifespan of X100CrMoV5 steel components operating in tribologically demanding environments.

Keywords: Coating, Hardness, TiN, TiAlN, TiAlSiN, Wear performance.

1. INTRODUCTION

The steady focus on enhanced tool longevity and machining efficiency remains one of the priorities in the manufacturing industry. One of the most prevalent and effective strategies employed to enhance the durability and performance of tool steels is the application of thin film coatings to their surfaces (Kumar and Choubey, 2024; Machado et al., 2024). This surface engineering approach aims to significantly improve the resistance of the tool to detrimental factors encountered during operation, such as wear, corrosion, and high temperatures, while preserving the mechanical properties of the base material. In this context, hard and chemically stable ceramic-based coatings, such as CrN (Kalin et al., 2024; Liu et al., 2024), TiN (Johny and Alphonse, 2024; Mandri et al., 2025), DLC (Barba et al., 2024; Grigoriev et al., 2025), AlTiN (Das et al., 2024; Brezinová et al., 2024), TiSiN (Agrawal et al., 2024), TiAlN (Da Silva et al., 2025; Tillmann et al., 2024), and TiAlSiN (Baskar et al., 2025; Lungu et al., 2024) are preferred surface modification materials in industrial applications. These coatings, owing to their high hardness, low coefficients of friction, and enhanced oxidation resistance, possess the potential to substantially improve the performance of tool steels used in various fields, including cutting and forming.

Among the various tool (mould) materials, X100CrMoV5 steel finds widespread use in the fabrication of moulds and dies for operations such as cold forging and stamping (Sommer, 2024; Theisen, 2008; Yang and Collins, 2003). However, even with its wear resistance, the demanding conditions encountered in these processes, characterized by high loads and sliding speeds, can lead to significant tool degradation, ultimately impacting product quality and production economics.

To reduce wear and extend the service life of X100CrMoV5 steel tooling, the deposition of hard, wear-resistant thin films has become increasingly prevalent. TiN has been extensively employed due to its high hardness, good adhesion to substrate, and relatively low cost (Mahajan et al., 2024). However, as manufacturing demands become more stringent, the limitations of TiN coatings (Naeem et al., 2022) have necessitated the exploration of more advanced coating systems. Ternary and quaternary nitride coatings, such as TiAlN and TiAlSiN, have garnered significant attention as promising alternatives. TiAlN represents a significant advancement, offering improved high-temperature performance and hardness. The incorporation of aluminium into the TiN lattice to form TiAlN has been shown to enhance oxidation resistance at elevated temperatures and improve hardness due to solid solution strengthening and the formation of a protective Al_2O_3 layer (Huang et al., 2025). TiAlSiN promises further enhancements in wear resistance and thermal stability. The addition of Si to the TiAlN system, resulting in TiAlSiN coatings, leads to further augment in hardness, thermal stability, and wear resistance by promoting the formation of a nanocomposite structure with amorphous Si_3N_4 grain boundaries that hinder dislocation movement and grain growth (Yin et al., 2024).

While the individual tribological properties of TiN, TiAlN, and TiAlSiN coatings on various substrates have been investigated in numerous studies, a comparative analysis of their wear behaviour specifically when deposited on X100CrMoV5 steel mould materials under systematically varied high-speed and high-load conditions remains pertinent. Understanding the performance characteristics of these coatings under conditions relevant to industrial metal forming processes is crucial for optimizing tool selection and maximizing operational efficiency.

This study aims to address this gap in knowledge by conducting a detailed investigation into the wear properties of TiN, TiAlN, and TiAlSi-coated X100CrMoV5 steels with a series of wear tests performed under a range of sliding speeds and applied loads, chosen to simulate the demanding conditions encountered in industrial mould applications. By providing a direct comparative assessment of the wear performance of these technologically important coatings on a widely used tool steel, this research seeks to provide valuable insights for tool designers and manufacturing engineers in selecting the most appropriate surface treatment for enhancing the durability and performance of X100CrMoV5 steel moulds operating under challenging tribological conditions.

The findings of this study are expected to contribute significantly to the advancement of surface engineering strategies for improving the efficiency and sustainability of metal forming processes.

2. MATERIALS AND METHODS

The chemical composition of the X100CrMoV5 steel substrate, as determined by optical emission spectrometry, is presented in Table 1. The chemical compositions of the TiN, TiAlN, and TiAlSiN coatings deposited onto the X100CrMoV5 steel substrates via physical vapour deposition process are given in Table 2.

Table 1. Chemical composition (wt.%) of X100CrMoV5 steel

	Chemical composition (wt.%)						
	C	Cr	Mo	V	Mn	Si	Fe
X100CrMoV5	0.99	5.08	1.05	0.24	0.53	0.27	Balanced

Table 2. Chemical compositions (wt.%) of TiN, TiAlN, and TiAlSiN coatings

	Chemical composition (wt.%)			
	Ti	N	Al	Si
TiN	50.28	49.72	–	–
TiAlN	26.34	47.49	26.17	–
TiAlSiN	18.60	43.78	33.85	3.77

The hardness of the TiN, TiAlN, and TiAlSiN coatings was evaluated using nanoindentation with a Berkovich indenter. Nanoindentation was chosen as the most appropriate method due to the thin nature of the coatings. Prior to testing, the coated specimens were carefully mounted in a cold mounting resin to provide stability. The surfaces were then prepared through a series of grinding and polishing steps using progressively finer grades of silicon carbide papers (P220 to P2500 grit) followed by polishing with diamond suspensions (3 µm and 1 µm). A Berkovich indenter, a three-sided pyramid with a known area function, was used to indent the TiN, TiAlN, and TiAlSiN coatings. A constant loading rate was applied to reach a peak load of 10 mN. The load was held at the peak value for 10 seconds, followed by a constant unloading rate to 5% of the peak load. A minimum of ten indentations were performed for each TiN TiAlN, and TiAlSiN-coated specimens.

The wear performance of the TiN, TiAlN, and TiAlSiN-coated X100CrMoV5 steel specimens was evaluated using a ball-on-disc tribometer according to the ASTM G99 standard. All wear tests were conducted under dry sliding conditions. The counterbody material consisted of a 6 mm diameter tungsten carbide-cobalt ball. An experimental design was employed to investigate the influence of two process parameters: the load and the sliding speed. Three distinct normal loads were applied to the coated surfaces: 2 N, 6 N, and 10 N. Correspondingly, three different sliding speeds were implemented: 0.1 m/s, 0.2 m/s, and 0.3 m/s at a sliding distance of 1000 meters. Prior to the initiation of each wear test, both the coated specimens and the tungsten carbide ball were cleaned in an ultrasonic bath containing ethanol for a duration of 10 minutes. This cleaning process was implemented to eliminate any surface contaminants that could potentially influence the frictional and wear behaviour.

Following the completion of wear tests on TiN, TiAlN, and TiAlSiN-coated X100CrMoV5 steel specimens, the obtained experimental data were subjected to a comprehensive analysis. The Design-Expert software was employed as the analytical tool for conducting the analysis of variance (ANOVA). This software also facilitated a detailed investigation into the impact of the factors, including the load and sliding speed, on the wear characteristics exhibited by the TiN, TiAlN, and TiAlSiN coatings.

3. RESULTS AND DISCUSSION

Figure 1 illustrates the hardness values of TiN, TiAlN, and TiAlSiN-coated X100CrMoV5 steels. The data reveals a clear trend in hardness, with the TiN coating exhibiting the lowest value, while the TiAlSiN coating demonstrated the highest values. Quantitative analysis indicates that the TiAlN and TiAlSiN coatings achieved hardness values that were approximately 1.36 and 1.6 times greater than that of the TiN coating, respectively.

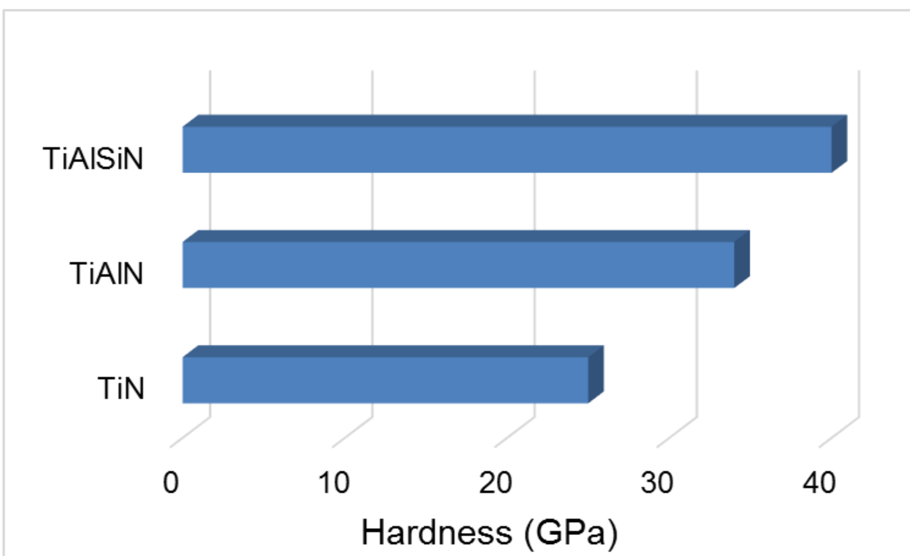

Figure 1. Hardness of TiN, TiAlN, and TiAlSiN-coated X100CrMoV5 steels

The enhanced hardness observed in TiAlN coating compared to the TiN coating can be attributed to several microstructural and compositional factors (Buranawong et al., 2011; He et al., 2024; Mayrhofer et al., 2003). The incorporation of aluminium into the titanium nitride lattice leads to a solid solution strengthening effect. The difference in atomic size between titanium and aluminium atoms introduces lattice strain, which impedes dislocation motion, the primary mechanism of plastic deformation in crystalline materials. This increased resistance to dislocation movement directly translates to higher hardness. Furthermore, the presence of aluminium promotes the formation of a more complex nitride structure, often exhibiting a finer grain size compared to TiN coatings deposited under similar conditions. According to the Hall-Petch relationship, materials with smaller grain sizes generally exhibit higher hardness due to the increased density of grain boundaries, which act as barriers to dislocation propagation (Das, S. et al. 2024). Additionally, the stronger Al-N bonds compared to Ti-N bonds contribute to the overall higher bond strength within the TiAlN matrix, further enhancing its resistance to indentation and thus its hardness. The formation of a denser and more compact microstructure in TiAlN coatings, which also plays a crucial role in its superior mechanical properties, including hardness. Fundamentally, the synergistic effects of solid solution strengthening, grain refinement, and the formation of stronger chemical bonds due to the incorporation of aluminium result in TiAlN coatings typically surpassing TiN coatings in terms of hardness.

The further augmentation of hardness observed in TiAlSiN coatings relative to TiAlN coatings is a consequence of intricate microstructural and compositional modifications arising from the incorporation of silicon (Kuptsov et al., 2015; Lü et al., 2020). The introduction of silicon into the TiAlN system promotes the evolution of a nanocomposite architecture. This structure characteristically comprises nanocrystalline TiAlN grains embedded within an amorphous or nanocrystalline silicon nitride (Si_3N_4) matrix (Kassymbaev et al., 2025). Several mechanisms contribute to the enhanced hardness inherent in this structural arrangement. Primarily, the presence of an amorphous Si_3N_4 phase at the boundaries of the TiAlN nanocrystallites serves as a potent impediment to dislocation mobility. As the primary mediators of plastic deformation in crystalline solids, the restricted movement of dislocations due to the surrounding amorphous network significantly elevates the resistance of the material to localized deformation under load, thereby increasing hardness. This phenomenon mirrors the grain boundary strengthening effect described by the Hall-Petch relationship, where a reduction in grain size correlates with increased hardness due to the greater interfacial area hindering dislocation movement. In the context of TiAlSiN, the continuous amorphous Si_3N_4 network effectively constrains the TiAlN nanocrystals, limiting their capacity for plastic deformation. Secondly, the inclusion of silicon can also induce solid solution strengthening within the TiAlN grains themselves (Kolchev et al., 2025). Silicon atoms occupying sites within the nitride lattice generate localized strain fields due to differences in atomic dimensions and electronic configurations. These strain fields interact with mobile dislocations, requiring a greater energy input for them to traverse the lattice, thus contributing to an overall increase in hardness. Thirdly, the development of the amorphous Si_3N_4 network enhances the thermal stability of the coating. This amorphous phase exhibits a high resistance to decomposition and grain growth at elevated temperatures. By effectively suppressing the coarsening of the TiAlN nanocrystals under thermal stress, the TiAlSiN coating is able to retain its refined microstructure and, consequently, its high hardness even in demanding thermal environments typical of industrial applications. In briefly, the combined effects of the unique nanocomposite structure, solid solution strengthening, and the improved thermal stability imparted by silicon integration lead to the consistently higher hardness values observed in TiAlSiN coatings when compared to TiAlN coatings.

A comprehensive overview of the experimental methodology, including the systematic design employed, the specific parameters investigated, and the corresponding experimental findings, the quantified wear rates, is presented in Tables 3−5. It should be noted that experiments 5, 6, and 7 in Tables 3–5 were repeated at the middle levels of load and sliding speed to estimate pure error and assess the linearity of the factor effects.

Table 3. Experimental design and the wear rate results of TiN-coated X100CrMoV5 steel as a function of load and sliding speed

Number of experiment	Type of coating	Coded value		Actual value		Wear rate [$(mm^3/N{\cdot}m){\cdot}10^{-7}$]
		Load	Sliding speed	Load (N)	Sliding speed (m/s)	
1	TiN	−1	−1	2	0.1	4.52
2	TiN	−1	0	2	0.2	5.36
3	TiN	−1	1	2	0.3	6.73
4	TiN	0	−1	6	0.1	5.05
5	TiN	0	0	6	0.2	6.08
6	TiN	0	0	6	0.2	6.22
7	TiN	0	0	6	0.2	5.96
8	TiN	0	1	6	0.3	8.23
9	TiN	1	−1	10	0.1	7.17
10	TiN	1	0	10	0.2	8.81
11	TiN	1	1	10	0.3	11.04

Table 4. Experimental design and the wear rate results of TiAlN-coated X100CrMoV5 steel as a function of load and sliding speed

Number of experiment	Type of coating	Coded value		Actual value		Wear rate [$(mm^3/N{\cdot}m){\cdot}10^{-7}$]
		Load	Sliding speed	Load (N)	Sliding speed (m/s)	
1	TiAlN	−1	−1	2	0.1	2.12
2	TiAlN	−1	0	2	0.2	2.50
3	TiAlN	−1	1	2	0.3	3.28
4	TiAlN	0	−1	6	0.1	2.64
5	TiAlN	0	0	6	0.2	3.15
6	TiAlN	0	0	6	0.2	3.24
7	TiAlN	0	0	6	0.2	3.30
8	TiAlN	0	1	6	0.3	4.31
9	TiAlN	1	−1	10	0.1	3.59
10	TiAlN	1	0	10	0.2	4.47
11	TiAlN	1	1	10	0.3	6.33

Table 5. Experimental design and the wear rate results of TiAlSiN-coated X100CrMoV5 steel as a function of load and sliding speed

Number of experiment	Type of coating	Coded value		Actual value		Wear rate [(mm^3/N·m)·10^{-7}]
		Load	Sliding speed	Load (N)	Sliding speed (m/s)	
1	TiAlSiN	−1	−1	2	0.1	1.91
2	TiAlSiN	−1	0	2	0.2	2.37
3	TiAlSiN	−1	1	2	0.3	2.86
4	TiAlSiN	0	−1	6	0.1	2.20
5	TiAlSiN	0	0	6	0.2	2.75
6	TiAlSiN	0	0	6	0.2	2.82
7	TiAlSiN	0	0	6	0.2	2.65
8	TiAlSiN	0	1	6	0.3	3.61
9	TiAlSiN	1	−1	10	0.1	2.98
10	TiAlSiN	1	0	10	0.2	3.84
11	TiAlSiN	1	1	10	0.3	5.03

In order to achieve a more in-depth understanding of the impact of load and sliding speed, and their combined effect, on the wear performance of TiN, TiAlN, and TiAlSiN-coated X100CrMoV5 steels, a detailed statistical investigation was carried out. This involved the application of both regression analysis and the analysis of variance (ANOVA) technique. These statistical methods were further utilized to evaluate the significance of the individual factors (load and sliding speed) and their interaction effect on the resulting wear rate and to validate the suitability of the developed predictive model.

The regression model exhibited high coefficients of determination (R^2), specifically 0.9976 for the TiN coating, 0.9947 for the TiAlN coating, and 0.9963 for the TiAlSiN coating as seen in Table 6. This indicates that over 99% of the total variance in wear rate could be statistically attributed to the investigated factors (load and sliding speed) and their interaction for each respective coating. It is generally understood that the predictive capability of the model strengthens as the R^2 value approaches unity. The adjusted R^2, a measure accounting for the number of predictors in the model and reflecting its goodness of fit to the observed data, was found to be 0.9951 for TiN, 0.9894 for TiAlN, and 0.9926 for TiAlSiN coating. Furthermore, the predicted R^2, which estimates the potential accuracy of the model in forecasting new, independent data points, was 0.9875 for TiN, 0.9528 for TiAlN, and 0.9793 for TiAlSiN coating.

Table 6. Fit statistics of regression model

	TiN coating	TiAlN coating	TiAlSiN coating
R^2	0.9976	0.9947	0.9963
Adjusted R^2	0.9951	0.9894	0.9926
Predicted R^2	0.9875	0.9528	0.9793

The statistical significance of the overall model was confirmed by a substantial F-statistic of 36.00 ($p < 0.001$) for TiN coating, 13.45 ($p < 0.001$) for TiAlN coating, and 7.63 ($p < 0.001$) for TiAlSiN coating. Concurrently, the lack-of-fit F-value was 1.06, 3.54, and 0.6280 with a corresponding p-value of 0.5181, 0.2282, and 0.6622 ($p > 0.05$) for TiN, TiAlN, and TiAlSiN coating, respectively, which was statistically non-significant. This non-significant lack of fit suggests a strong agreement between the predictions of the model and the experimental observations, supporting the reliability of the model for predicting the wear rate response under varying conditions of load and sliding speed parameters. The significance of a term in influencing the response was determined based on its p-value, with a threshold of $p < 0.05$ corresponding to a 95% confidence level. As detailed in Tables 7−9, the p-values for the linear terms of load and sliding speed, and the quadratic terms of load*load and sliding speed*sliding speed and interaction term of load*sliding speed were all below 0.05. Given that all these p-values are below the significance level of 0.05, it can be concluded that these terms had a statistically significant effect on the wear rate of TiN, TiAlN, and TiAlSiN-coated X100CrMoV5 steels.

188

Table 7. Analysis of variance (ANOVA) for wear rate depending on the factors of load and sliding speed for TiN-coated X100CrMoV5 steel

Source	Sum of Squares	df	Mean Square	F-value	p-value	
Model	36.00	5	7.20	409.61	< 0.0001	significant
Load	18.06	1	18.06	1027.54	< 0.0001	
Sliding speed	14.29	1	14.29	813.06	< 0.0001	
Load*Sliding speed	0.6889	1	0.6889	39.19	0.0015	
Load*Load	1.85	1	1.85	105.23	0.0002	
Sliding speed*Sliding speed	0.4248	1	0.4248	24.17	0.0044	
Residual	0.0879	5	0.0176			
Lack of Fit	0.0540	3	0.0180	1.06	0.5181	not significant
Pure Error	0.0339	2	0.0169			
Cor Total	36.09	10				

Table 8. Analysis of variance (ANOVA) for wear rate depending on the factors of load and sliding speed for TiAlN-coated X100CrMoV5 steel

Source	Sum of Squares	df	Mean Square	F-value	p-value	
Model	13.45	5	2.69	187.08	< 0.0001	significant
Load	7.02	1	7.02	488.30	< 0.0001	
Sliding speed	5.17	1	5.17	359.67	< 0.0001	
Load*Sliding speed	0.6241	1	0.6241	43.41	0.0012	
Load*Load	0.2397	1	0.2397	16.68	0.0095	
Sliding speed*Sliding speed	0.2244	1	0.2244	15.61	0.0108	
Residual	0.0719	5	0.0144			
Lack of Fit	0.0605	3	0.0202	3.54	0.2282	not significant
Pure Error	0.0114	2	0.0057			
Cor Total	13.52	10				

Table 9. Analysis of variance (ANOVA) for wear rate depending on the factors of load and sliding speed for TiAlSiN-coated X100CrMoV5 steels.

Source	Sum of Squares	df	Mean Square	F-value	p-value	
Model	7.63	5	1.53	269.20	< 0.0001	significant
Load	3.70	1	3.70	652.03	< 0.0001	
Sliding speed	3.24	1	3.24	571.61	< 0.0001	
Load*Sliding speed	0.3025	1	0.3025	53.35	0.0008	
Load*Load	0.2685	1	0.2685	47.34	0.0010	
Sliding speed*Sliding speed	0.0399	1	0.0399	7.04	0.0453	
Residual	0.0284	5	0.0057			
Lack of Fit	0.0138	3	0.0046	0.6280	0.6622	not significant
Pure Error	0.0146	2	0.0073			
Cor Total	7.66	10				

Table 10 shows the coefficients of linear (load and sliding speed), quadratic (load*load and sliding speed*sliding speed) and interaction (load*sliding speed) terms of factors influencing the wear rate. The coefficients presented in Table 10 quantify the influence of each term on the wear rate. Notably, the coefficient associated with the load parameter exhibited a higher level than that of the sliding speed. This observation signifies that the applied load had a greater impact on the wear performance of the TiN, TiAlN, and TiAlSiN-coated X100CrMoV5 steels compared to the sliding speed within the investigated range.

Table 10. Coefficients of linear (load and sliding speed), quadratic (load*load and sliding speed*sliding speed) and interaction terms (load*sliding speed) of factors influencing the wear rate.

Factor	Coefficient Estimate		
	TiN	TiAlN	TiAlSiN
Intercept	6.14	3.21	2.76
Load	1.74	1.08	0.7850
Sliding speed	1.54	0.9283	0.7350
Load*Sliding speed	0.4150	0.3950	0.2750
Load*Load	0.8545	0.3076	0.3255
Sliding speed*Sliding speed	0.4095	0.2976	0.1255

Figure 2 presents the main effect of load and sliding speed on the wear rate of TiN, TiAlN, and TiAlSiN-coated X100CrMoV5 steels. The wear rate was significantly affected by both factors, increasing with higher load and sliding speed for all coatings. The load demonstrated a higher influence on the wear rate compared to the sliding speed. As depicted in Figure 2, the TiAlSiN coating exhibited the lowest wear rate among the tested coatings. This observation indicates that the application of the TiAlSiN coating resulted in a significant improvement in the wear resistance of the X100CrMoV5 steel substrate compared to both the TiN and TiAlN coatings. The superior wear resistance of the TiAlSiN coating can be attributed to several factors, including its higher hardness.

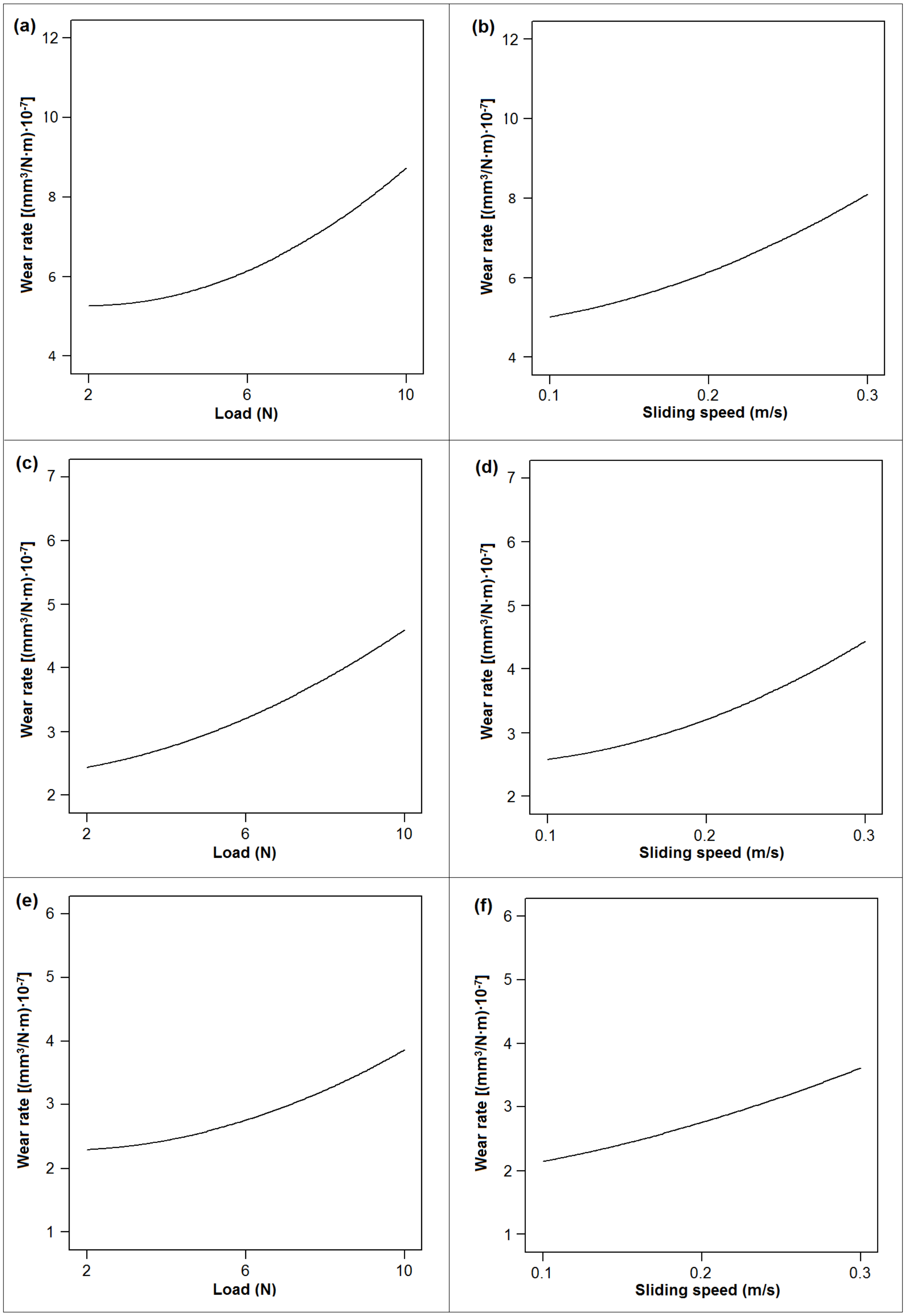

Figure 2. Main effect of load and sliding speed on the wear rate of the TiN ((a) and (b)), TiAlN ((c) and (d)), and TiAlSiN ((e) and (f)) coated X100CrMoV5 steels

To provide a better understanding of the relationships, three-dimensional response surface curves and two-dimensional contour charts are utilized. These visuals effectively illustrate the interaction effect of the factors on the response. Figures 3–5 show the impact of load and sliding speed and their interaction on the wear rate of TiN, TiAlN, and TiAlSiN-coated X100CrMoV5 steels. Consistent with the ANOVA results, the interaction between load and sliding speed was statistically significant on the wear rate. An increase in both load and sliding speed led to a corresponding increase in the wear rate of the TiN, TiAlN, and TiAlSiN coatings. It is important to note that the wear rate accelerated at higher load and sliding speed values. Furthermore, the more pronounced influence of increasing load on the wear rate, compared to an equivalent increase in sliding speed, can likely be attributed to the greater stress and temperature generated under higher load conditions.

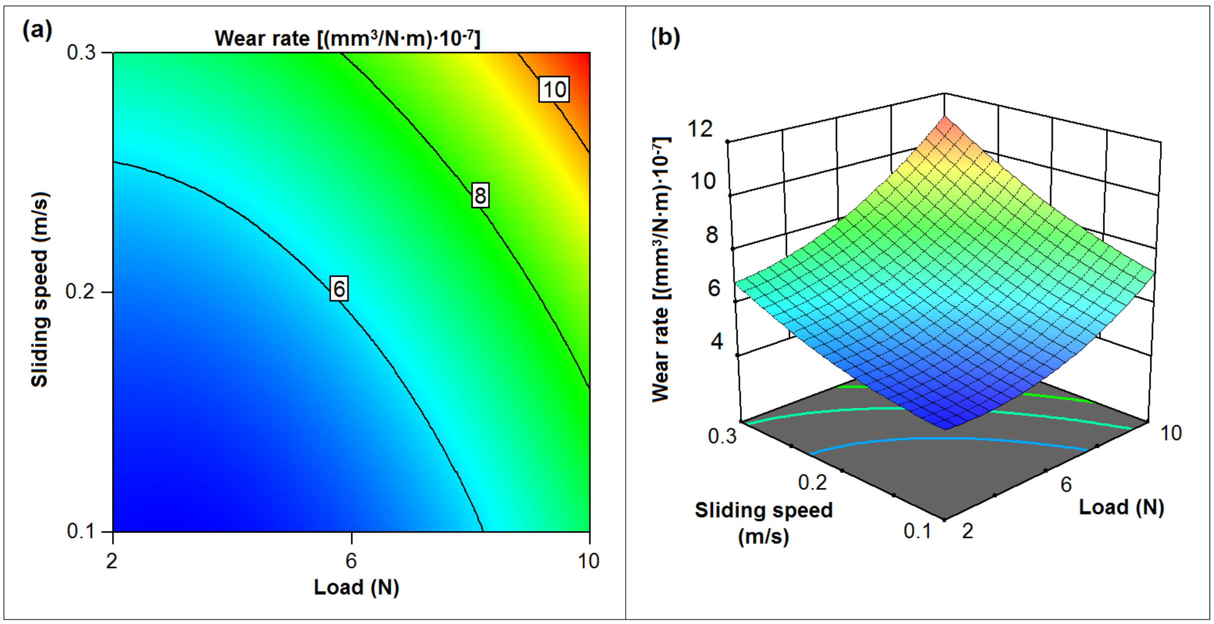

Figure 3. (a) Two-dimensional contour plot and (b) Three-dimensional response surface plot showing the interaction effect between load and sliding speed on the wear rate of the TiN-coated X100CrMoV5 steel.

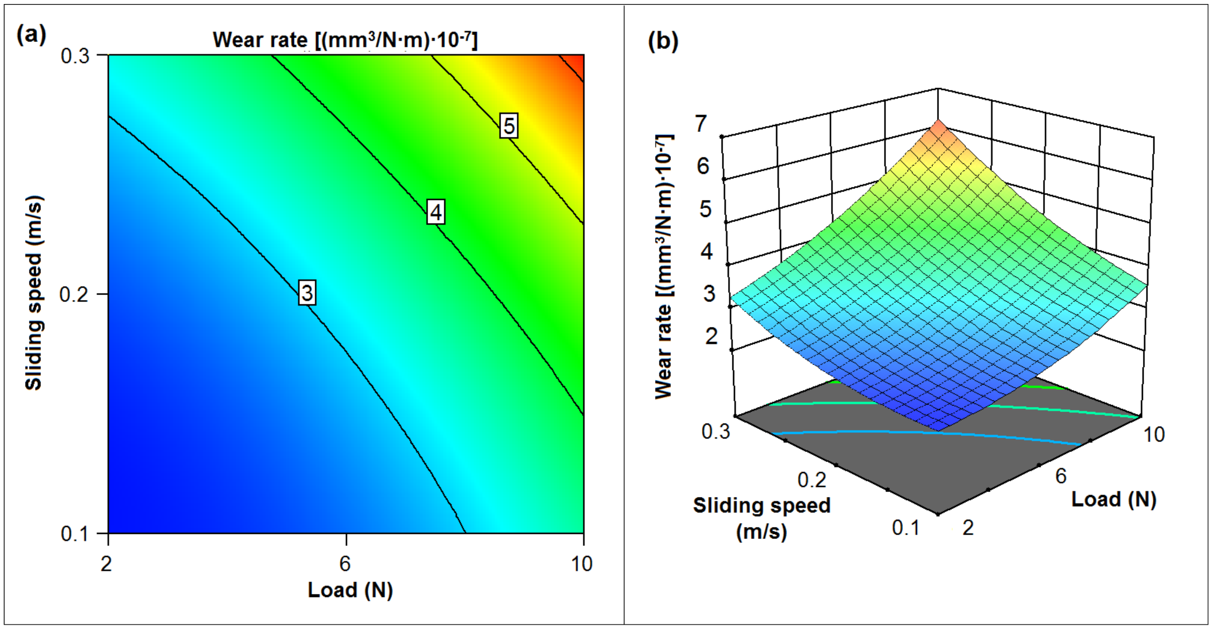

Figure 4. (a) Two-dimensional contour plot and (b) Three-dimensional response surface plot showing the interaction effect between load and sliding speed on the wear rate of the TiAlN-coated X100CrMoV5 steel.

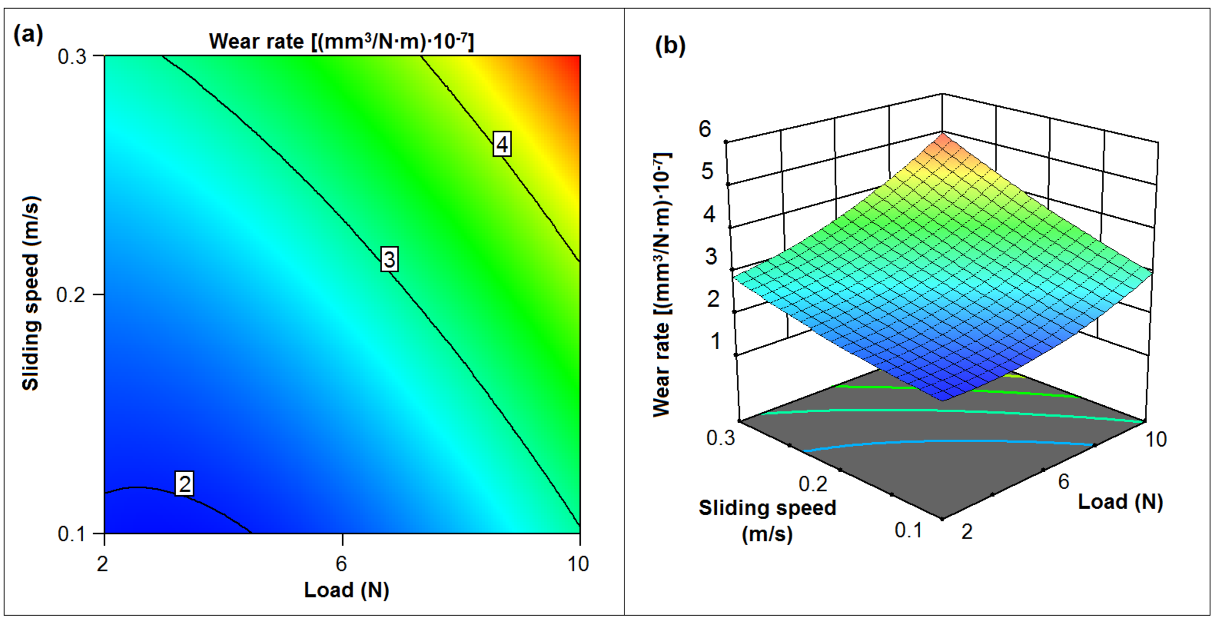

Figure 5. (a) Two-dimensional contour plot and (b) Three-dimensional response surface plot showing the interaction effect between load and sliding speed on the wear rate of the TiAlSiN-coated X100CrMoV5 steel.

The observed wear behaviour suggests that the TiAlSiN coating offers a considerable advantage in terms of wear resistance for the X100CrMoV5 steel compared to the TiN and TiAlN coatings. This enhanced performance likely stems from the unique properties of the TiAlSiN coating, such as its increased hardness, which contributed to a lower material removal rate during the wear tests.

4. CONCLUSIONS

This study investigated the wear performance of TiN, TiAlN, and TiAlSiN-coated X100CrMoV5 steels under varying conditions of applied load and sliding speed. The quantitative analysis of hardness revealed a progressive increase for the coating materials, with TiAlSiN exhibiting the highest value, followed by TiAlN, and then TiN. The TiAlN and TiAlSiN coatings achieved hardness values that were approximately 1.36 and 1.6 times greater than that of the TiN coating, respectively.

Comparative analysis of the wear rates revealed that the TiAlSiN coating consistently exhibited the lowest wear rate across the range of tested loads and sliding speeds. This superior wear performance signifies a substantial enhancement in the wear resistance of the X100CrMoV5 steel substrate when protected by the TiAlSiN coating, outperforming both the TiN and TiAlN coatings. This improved wear behaviour is a direct consequence of the higher hardness of the TiAlSiN coating, which provides greater resistance to plastic deformation and material removal during the tribological testing.

Statistical modelling through regression analysis and ANOVA demonstrated a strong correlation between the investigated factors (load and sliding speed) and the wear rate for all three coatings, with R^2 values exceeding 0.99. Both load and sliding speed were found to have a statistically significant influence on the wear rate, with a clear trend of increasing wear with increasing parameter values. Notably, the applied load exhibited a more pronounced effect on the wear rate compared to the sliding speed. Furthermore, the interaction between load and sliding speed was also found to be statistically significant, indicating a non-linear relationship where the combined effect of these parameters on wear rate is greater than the sum of their individual effects, particularly at higher values.

In conclusion, the findings of this study underscore the significant impact of coating composition on the wear performance of X100CrMoV5 steel. The TiAlSiN coating demonstrated a clear advantage in terms of hardness and wear resistance compared to TiN and TiAlN coatings under the investigated conditions. This suggests that TiAlSiN coatings offer a promising surface modification strategy for enhancing the durability and extending the service life of X100CrMoV5 steel components subjected to demanding wear environments. Further research could explore the long-term wear behaviour and performance of these coatings under more complex and application-specific conditions.

References

Agrawal, P., Kenche, S., Kumar, T. S. (2024). Drilling performance analysis on super duplex stainless steel (AISI 2507) using scalable pulse power plasma TiSiN- and AlTiN-coated tools and optimizing machining parameters through Taguchi–Fuzzy approach. Proceedings of the Institution of Mechanical Engineers. Part E: Journal of Process Mechanical Engineering, In press. https://doi.org/10.1177/09544089241270849.

Barba, E., Claver, A., Montalà, F., Palacio, J.F., Luis-Pérez, C. J., Sala, N., Colominas, C., García, J. A. (2024). Study of the industrial application of diamond-like carbon coatings deposited on advanced tool steels. Coatings, 14(2), 159.

Baskar, S., Raman, A., Karthick, M., Lenin, N., Rajesh, K., Rohini, B., Chandrasekaran, M., Uma, D. A., Sudharsan, M. S., Ruban, M. (2025). Enhancing machining efficiency of UNS S45000 alloy steel using cryogenically treated TiAlSiN coated tungsten carbide inserts. Results in Engineering, 25, 104415.

Brezinová, J., Džupon, M., Puchý, V., Brezina, J., Maruschak, P., Guzanová, A., Sobotová, L., Badida, M. (2024). Research on the tribological properties of a new generation of multi-layer nanostructured PVD coatings for increasing the technological lifetime of moulds. Metals, 14(1), 131.

Buranawong A., Witit-anun, N., Chaiyakun, S., Pokaipisit, A., Limsuwan, P. (2011). The effect of titanium current on structure and hardness of aluminium titanium nitride deposited by reactive unbalanced magnetron co-sputtering. Thin Solid Films, 519(15), 4963–4968.

Da Silva, S. P., Abrão, A. M., da Silva, E. R., Câmara, M. A. (2025). Enhanced wear resistance and frictional behavior of AISI H13 tool steel through in-situ urea-assisted EDM nitriding and TiAlN PVD coating. The International Journal of Advanced Manufacturing Technology, 138, 2459–2473.

Das, A., Kumar, A., Padhan, S., Das, S. R. Satpathy, M. P., Patel, S. K. (2024). Hard turning of AISI H10 steel using AlTiN and AlTiSiN coated carbide tools: comparative machining performance evaluation and economic assessment. Journal of the Brazilian Society of Mechanical Sciences and Engineering, 46, 277.

Das, S., Biswas, S. K., Kundu, A., Ghadai, R., Guha, S. (2024). Investigation of mechanical morphological structural and electrochemical properties of PVD TiAlN coating: A detail experimental and its correlation with an analytical approach using the least square method. Applied Surface Science Advances, 24, 100638.

Grigoriev, S. N., Volosova, M. A., Korotkov, I. A., Gurin, V. D., Mitrofanov, A. P., Fedorov, S. V., Okunkova, A. A. (2025). Increasing the wear resistance of stamping tools for coordinate punching of sheet steel using CrAlSiN and DLC:Si coatings. Technologies, 13, 30.

He, Q. Sun, T. Y., Huang, L. F. (2024). Chemical-bonding and lattice-deformation mechanisms unifying the stability and diffusion trends of hydrogen in TiN and AlN polymorphs. Acta Materialia, 281, 120447.

Huang, P. Y., Liang, Y. C., Tsai, C. L., Hung, C. F., Yeh, J. W., Tsai, C. W. (2025). Mechanical, anti-oxidation and cutting performance of AlBCCrNbSi high entropy nitride coatings with various substrate bias. Surface and Coatings Technology, 511, 132267.

Johny, B. S., Alphonse, M. (2024). Friction and wear behaviour of AlCrN and TiN coated H13 tool steel. Tribology and Materials, 3(3), 131–140.

Kalin, M., Jerina, J,. Sharma, S. K., Kovač, J. (2024). The effect of temperature on the transfer layer of an aluminium alloy on tool steel and the effect of CrN coating. Tribology - Materials, Surfaces & Interfaces, 18(1), 11–19.

Kassymbaev, A., Myakinin, A., Uazyrkhanova, G., Belisarova, F., Sagidugumar, A., Kimossov, R. (2025). Influence of thickness on the structure and properties of TiAl(Si)N gradient coatings. Coatings, 15, 710.

Kolchev, S., Kolaklieva, L., Kovacheva, D., Atanasova, G., Cholakova, T., Chitanov, V., Zlatareva, E., Kakanakov, R., Pashinski, C. (2025) Mechanical and tribological behavior of TiAlSiN/AlSiN coatings depending on the high-temperature treatment. Coatings, 15, 542.

Kumar, N., Choubey, V. K. (2024). Recent trends in coating processes on various AISI steel substrates: A review. Journal of Materials Science, 59, 395–422.

Kuptsov, K. A., Kiryukhantsev-Korneev, Ph. V., Sheveyko, A. N., Shtansky, D. V. (2015). Structural transformations in TiAlSiCN coatings in the temperature range 900–1600°C. Acta Materialia, 83, 408–418.

Liu, Y., Yang, Y., Liu, X., Zheng, J., Zhang, S. (2024). Tribocorrosion of CrN coatings on different steel substrates. Surface and Coatings Technology, 484, 130829.

Lungu, M. V., Tălpeanu, D., Ciobanu, R. C., Cojocaru, A., Pătroi, D., Marinescu, V., Caramitu, A. R. (2024). Evaluation of magnetron sputtered TiAlSiN-based thin films as protective coatings for tool steel surfaces. Coatings, 14(9), 1184.

Lü, W., Li, G., Zhou, Y., Liu, S., Wang, K., Wang, Q. (2020). Effect of high hardness and adhesion of gradient TiAlSiN coating on cutting performance of titanium alloy. Journal of Alloys and Compounds, 820, 153137.

Machado, A. R., da Silva, L. R. R. Pimenov, D. Y., de Souza, F. C. R., Kuntoğlu, M., de Paiva, R. L. (2024). Comprehensive review of advanced methods for improving the parameters of machining steels. Journal of Manufacturing Processes, 125, 111–142.

Mahajan, U., Dhonde, M., Sahu, K., Ghosh, P., Shirage, P. M. (2024). Titanium nitride (TiN) as a promising alternative to plasmonic metals: a comprehensive review of synthesis and applications. Materials Advances, 5, 846−895.

Mandri, A. D., Colombo, D. A., Sanchez, N. V., Brühl, S. P., Dommarco, R. C. (2025). Rolling contact fatigue of ion nitrided and TiN coated AISI 4140 steel under pure rolling condition. Engineering Failure Analysis, 170, 109311.

Mayrhofer, P. H., Hörling, A., Karlsson, L., Sjölén, J., Larsson, T., Mitterer, C., Hultman, L. (2003). Self-organized nanostructures in the Ti–Al–N system. Applied Physics Letters, 3, 2049–2051.

Naeem, M., Awan, S., Shafiq, M., Raza, H. A., Iqbal, J., Díaz-Guillén, J. C., Sousa, R. R. M., Jelani, M., Abrar, M. (2022). Wear and corrosion studies of duplex surface-treated AISI-304 steel by a combination of cathodic cage plasma nitriding and PVD-TiN coating. Ceramics International, 48(15), 21473−21482.

Sommer, P. (2024). Manufacturing influence area after heat treatment. In: Mistakes before, during and after heat treatment of steel. Springer.

Theisen, W. (2008). Tools for processing materials. In H. Berns, W. Theisen (Eds.), Ferrous Materials. Springer.

Tillmann, W., Meijer, A. L., Platt, T., Biermann, D., Stangier, D., Dias, N. F. L. (2024). Cutting performance of TiAlN-based thin films in micromilling high-speed steel AISI M3:2. Manufacturing Letters, 40, 6−10.

Yang, L. J., Collins, D. N. (2003). Designing with tool steel. In G. E. Totten, L. Xie, K. Funatani (Eds.), Handbook of mechanical alloy design. CRC Press.

Yin, Z., Wu, S., Zhang, Y., Yan, W., Dai, S., Peng, X., Liao, B., Zhang, X., Wang, J., Ouyang, X., Chen, L., Ouyang, X. (2024). A comparative study on the structure and properties of TiAlSiN coatings deposited by FCVA and HiPIMS. Journal of Alloys and Compounds, 1005, 175844.